



LAWRENCE
LIVERMORE
NATIONAL
LABORATORY

An Experimental Investigation of Detonation Corner-Turning Using High Resolution Radiography

J. D. Molitoris, H. G. Andreski, R. G. Garza, J. D.
Batteux, P. C. Souers

July 20, 2006

13th International Detonation Symposium
Norfolk, VA, United States
July 23, 2006 through July 28, 2006

Disclaimer

This document was prepared as an account of work sponsored by an agency of the United States Government. Neither the United States Government nor the University of California nor any of their employees, makes any warranty, express or implied, or assumes any legal liability or responsibility for the accuracy, completeness, or usefulness of any information, apparatus, product, or process disclosed, or represents that its use would not infringe privately owned rights. Reference herein to any specific commercial product, process, or service by trade name, trademark, manufacturer, or otherwise, does not necessarily constitute or imply its endorsement, recommendation, or favoring by the United States Government or the University of California. The views and opinions of authors expressed herein do not necessarily state or reflect those of the United States Government or the University of California, and shall not be used for advertising or product endorsement purposes.

AN EXPERIMENTAL INVESTIGATION OF DETONATION CORNER-TURNING USING HIGH RESOLUTION RADIOGRAPHY

John D. Molitoris, Henry G. Andreski, Raul G. Garza, Jan D. Batteux, P. Clark Souers

Energetic Materials Center / Lawrence Livermore National Laboratory
University of California, Livermore, CA, 94551 USA

Abstract. We have performed experiments investigating detonation corner turning over a range of high-explosives including LX-17, Composition B, LX-04 and Tritonal. The primary diagnostic utilized here was a new high-resolution x-ray system that was capable of recording a time sequence of the detonation process as it negotiated the corner of interest and propagated. For LX-17 our data detail the formation of a significant dead-zone. Although the detonation eventually turned the corner in LX-17, the dead zone persisted to late times and evidence exists that it never was consumed by either detonation or fast combustion processes. In LX-17 the detonations ability to corner-turn increases as the density is reduced. Furthermore, lowering the density decreases the size of the dead-zone and alters its shape. The other high-explosives investigated were able to turn the corner immediately with no indication of any dead-zone formation.

INTRODUCTION

These experiments were designed to investigate detonation corner-turning in any high explosive. The experimental configuration utilizes an external corner/air well by mating a small diameter booster column to a larger diameter main charge. The connection between the booster and the main charge establishes the corner that the detonation must negotiate. Due to the physical resemblance, this experimental set-up is known as a German Hand Grenade or GHG configuration. Cox and Campbell have previously used this configuration to study corner turning in PBX 9502 [1]. They concluded that the explosive had a 17 mm corner-turning radius and that the material inside this radius did not detonate. Manfred Held [2,3] has since refined this geometry into a test for corner-turning and first used the term "dead-zone" to describe the region of unreacted explosive.

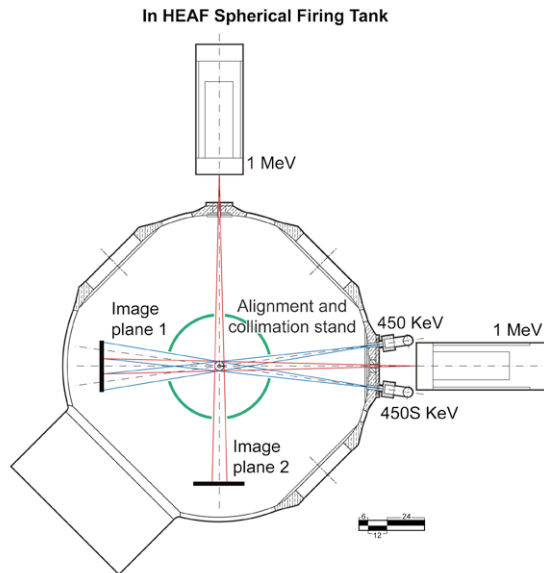
Corner-turning and dead-zone formation in TATB based high explosives has also recently been studied by Souers et al [4]. Souers used an internal air-well geometry also known as a hockey puck configuration. In this work a unique high-resolution radiography system was used to image the dead-zone [5]. More recent work by Souers et. al [6], mentions some of the results noted here. In this paper we show and discuss the full set of GHG corner-turning radiographic data taken for LX-17 (92.5% TATB, 7.5% kel-F), Composition B (60% RDX, 40% TNT), LX-O4 (85% HMX, 15% Viton A), and Tritonal (80% TNT, 20% Aluminum).

EXPERIMENTAL

All data reported in this paper were taken with the Hydra multi-channel x-ray diagnostic which operates in the HEAF spherical firing tank. Hydra typically takes four images per high-explosive shot. This diagnostic has higher x-ray flux per imaging

channel, better image contrast, more precise timing, and better spatial resolution than its predecessor described in reference 4.

Figure 1 schematically shows the layout of the Hydra diagnostic in the spherical firing tank. The diagnostic takes advantage of the cylindrical symmetry of these experiments to record a four-image time sequence for each shot.



4 x-ray channels: 2 – 1 MeV Super, 1 – 450 KeV Super, 1 – 450 KeV

FIGURE 1. Four channel set-up of the Hydra X-Ray diagnostic as configured for these experiments.

The basic principle used here is point projection radiography. The x-rays are projected from point sources outside the firing tank through thin aluminum windows. The x-rays are heavily collimated before passing through the object plane, an explosive experiment at the center of the firing tank. Each x-ray channel projects a distinct non-overlapping image on to a multiple plane film pack. In these experiments Hydra was actually used in two different configurations. A two-channel mode making use of only the orthogonal 1 MeV units and a four-channel mode as illustrated in the figure shown. Magnification was typically 1.2X to 1.3X. A temporal resolution of 25 ns was defined by the flash duration and was constant for all shots. Spatial resolution varied due to changes in contrast, but was typically from 0.1 mm to 0.5 mm. As each of the four channels can be independently triggered

(flash time jitter is less than 100 ns and usually 50 ns) on a specific shot, a time sequence of up to four images can be obtained on the same shot/experiment. In addition to the collimation, the film packs are shielded so that cross-projections are not possible.

Radiation dose is over 10 grays for the two 1 MeV x-ray channels, about 7 grays for the 450S channel, and 5 grays for the 450 channel. This is the radiation dose per pulse at 1 m with 0.4 mm full-width-half-maximum spot size. The high dose channels of Hydra consist of two Super 1 MeV Pulsers while the lower dose channels consist of a Super 450 KeV pulser and a regular 450 KeV pulser. All super pulsers are modified to generate higher flux and hence higher dose. Referencing the figure, the two 1 MeV channels are at 90 degrees to each other. The 450 units are 8 degrees to either side of one of the MeV unit forming a close cluster of images. All units project images that are well separated compound film packs.

Image contrast can be optimized by adjusting the pulser high-voltage and/or the film pack configuration. As the voltages can be adjusted separately, the MeV and 450 KeV channels can be individually optimized for a given experiment. This gives Hydra a high degree of flexibility to be optimized for a very wide range of experiments. The multi-plane film packs allow up to six images of varying sensitivity to be taken per channel. This allows us to image a wide range of densities per shot and combine or subtract images to bring out the details of interest.

As the charges for the GHG experiments were small (less than 300 g) and uncased, the film packs could be placed very close to the object for very high contrast and definition. This is the reason the first set of experiments was run in a two-channel mode. In this mode we are only using the center channel of the cluster, so overlap is not an issue. Ultimately we were able to fine tune the system so that the four-channel mode produced data of equal or even better quality for these experiments.

As the “hockey-puck” experiment configuration used in references 4 and 6 requires relatively complex machined explosive components, the GHG configuration was ideal for performing a large number of shots at reduced cost. Figure 2 below shows a schematic of the GHG configuration. The handle component was usually a stack of high explosive pellets about 2.5 inches in

length. LX-14 (95% HMX, 5% estane) was our primary booster/handle material and used for most of the shots, but for some shots pentolite, Composition B and Octol were used as boosters. Most of the boosters were 0.5 inches in diameter. The largest portion of the final data set kept the ratio of main charge diameter to handle diameter at 4:1.

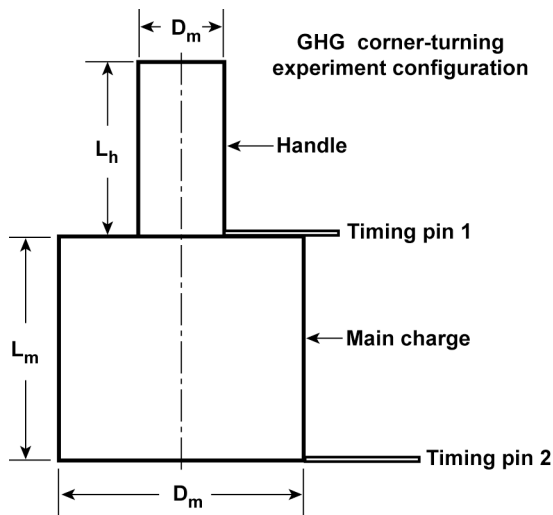


FIGURE 2. GHG experiment configuration in these experiments.

The timing pins shown in the figure were critical to the experiment. Due to detonation time jitter, we used a crystal pin to define the zero or start time for the corner turning event. The crystal pin notes the detonation arrival at the surface of the main charge, so we had a clear timing fiducial in these experiments. The second timing pin was used as a check to determine the overall detonation transit time in the main charge. Digitizing oscilloscopes recorded the detonator current start, bridgewire burst time, pin times, and the firing time of the x-ray channels. All times quoted below are in relation to timing pin 1.

RESULTS AND DATA REDUCTION

A summary of all shots reported here is tabulated in Table 1 below. All charges were uncased and at ambient temperatures when detonated. Most of the experiments were done with LX-17 as the main charge, followed by Composition B. Single experiments were done on LX-04 and Tritonal. The first six experiments were

performed with the Hydra diagnostic in a 2-channel mode while the rest of the series utilized the 4-channel mode. X-ray flash times measured post-pin as discussed above ranged from 0.810 us to almost 22 us. We tried to keep the main charge to booster diameter ratio at 4:1, but in some cases this was not possible. We also endeavored to keep the handle length at 2.5 inches, but some experiments were done with booster handles as short as 1 to 1.5 inches. We are skeptical of the experiments utilizing shorter handles as the initiating shock/detonation may not be in steady state and have a higher curvature. Main charge initiation from a detonation with a higher degree of curvature would certainly impact our measurements. In summary, we have seven shots performed in an identical geometry (4:1 diameter ratio with 2.5 inch long initiator) and six shots which were close to it.

The data presented below are in image form. In all of the raw data the detonation front is always apparent along with the dead-zone (if it is formed). We apply an Abel inversion technique [7] in some cases to determine local density (in three-dimensions) from these line-of-sight measurements. This technique has previously been used by Aufderheide [8] to perform tomographic reconstruction of detonating materials in density space. The Abel technique effectively reconstructs the three-dimensional object from the two-dimension image projected on the film plane assuming a true cylindrical symmetry. It then produces a true slice of the 3D image for analysis. If the feature of interest is sufficiently removed from the axis of symmetry and data not too noisy, the reconstruction works well. This technique fails for features near the central axis and degrades as noise in the data increases. Finally artifacts in the image (scratches, wires, etc.) if not removed or filtered out are amplified during the reconstruction.

In many cases below the Abel technique has allowed us to further enhance the distinctiveness of the detonation front and dead-zone.

LX-04 Results

As LX-04 is 85% HMX and the 1.860 g/cc density of the pressed main charge evaluated here is well below the theoretical maximum density (TMD) of 1.896 g/cc, we expected no corner turning issues. We lead off the discussion of our results with LX-04 as these data provide a

Table 1. Summary of experimental data.

GHG Shot Summary								
	Shot	Description	Main Charge		Density g/cc	Handle		
			HE	Dia × Len		HE	Dia × Len	Total length
1	GHG-04-001	Cast	Tritonal	3 × 2.5	1.710	Pentolite	1 × 1; 3 × .75	1
2	GHG-04-002	Pressed	LX-17	2 × 2	1.910	Comp B	1 × 1	1
3	GHG-04-003	Pressed	LX-17	2 × 2	1.910	LX-14	0.5 × 0.5 (5)	2.5
4	GHG-04-004	Pressed	LX-17	2 × 2	1.870	LX-14	0.5 × 0.5 (5)	2.5
5	GHG-04-005	Pressed	Comp B	2 × 2	1.700	LX-14	0.5 × 0.5 (5)	2.5
6	GHG-04-006	Pressed	LX-04	2 × 2	1.860	LX-14	0.5 × 0.5 (5)	2.5
7	GHG-04-007	Cast	Comp B	1.5 × 3	1.590	LX-14	0.5 × 0.5 (5)	2.5
8	GHG-04-008	Pressed	LX-17	2 × 2	1.908	LX-14	0.5 × 0.5 (5)	2.5
9	GHG-04-009	Pressed	LX-17	2 × 2	1.908	LX-14	0.5 × 0.5 (5)	2.5
10	GHG-04-010	Pressed	LX-17	2.5 × 2.2	1.909	OCTOL	1 × 1 (2)	2
11	GHG-05-001	Pressed	LX-17	2 × 2	1.908	LX-14	1 × 1 (3)	3
12	GHG-05-002	Pressed	LX-17	2 × 2	1.909	LX-14	0.5 × 0.5 (3)	1.5
13	GHG-05-003	Cast	Comp B	3.86 × 5	1.590	Comp B	1 × 1 (2)	2

Notes: All dimensions in inches.
Numbers in parenthesis are number of elements in handle stack.

good basis of comparison with the other explosives. Figure 3 below shows the LX-04 time sequence starting with a static radiograph. Figure 3b) was imaged 1.91 us and shows a clean dish-shaped detonation nearly breaking-out of the main charge. Figure 3c) is taken 2 us later and shows a typical detonation front in a cylindrical charge with no evidence of a dead-zone. These data are in stark contrast to that taken for LX-17.

LX-17 Results

All LX-17 experiments showed an inability of the detonation to turn the corner and resulted in dead-zone formation. Even the second experiment in the series (see table 1) where the cylinder ratio

was 2:1 with a one inch long booster was unable to effectively corner turn. Figure 4 below illustrates typical features in an LX-17 experiment. The left hand figure is a raw data image. Here we point out the detonation front and the dead-zones. This image was taken after detonation had effectively turned the corner and after detonation breakout. The image on the right hand side is the same data, but Abel inverted. In the Abel image the dead-zones and detonation front are clearer and more distinct. The Abel routine does add noise, especially at small radii. These figures should be compared to Figure 3c), which was taken at about the same time. Most of the LX-17 main charges were 1.910 g/cc.

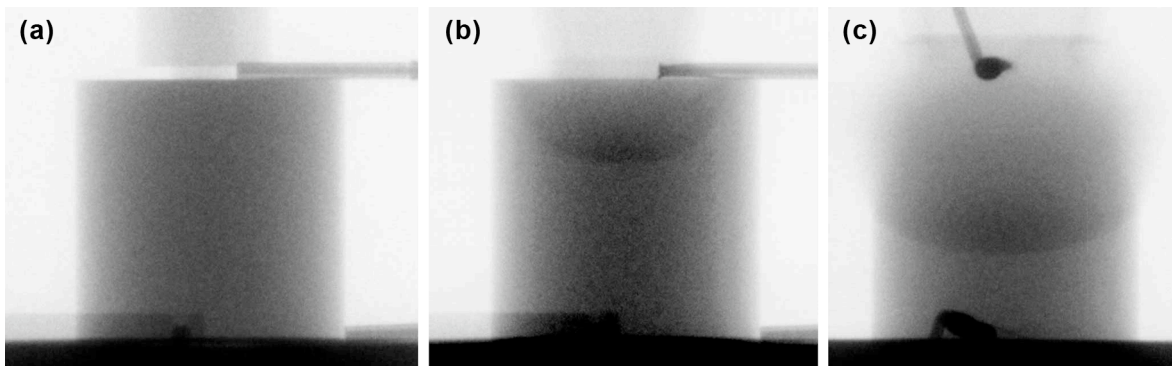


Figure 3. LX-04 detonation sequence; a) static; b) 1.91 us; c) 3.90 us.

Corner Turning and Dead Zone Formation in LX-17

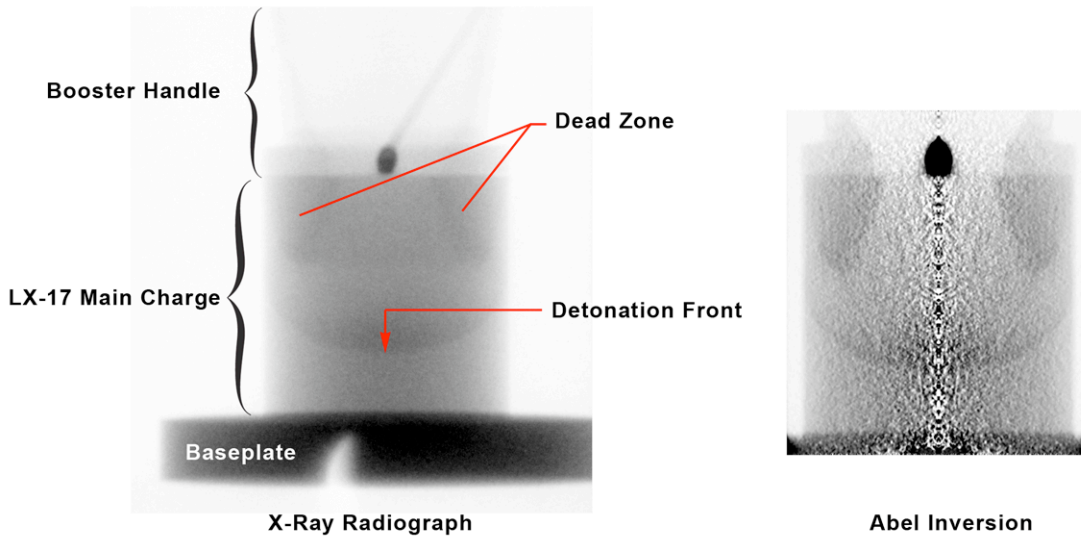


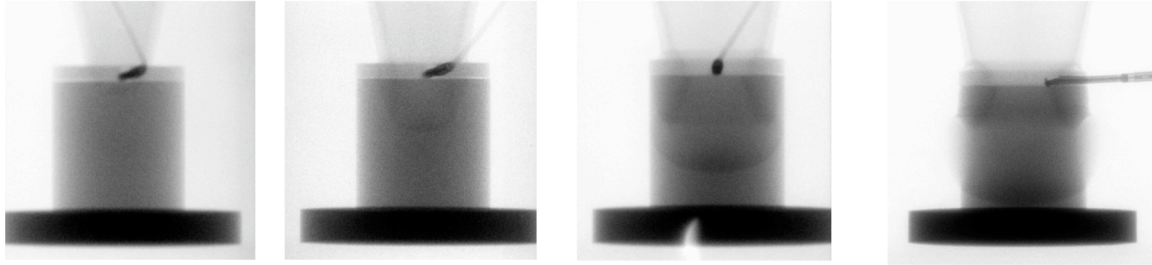
Figure 4. Radiographic image (LHS) and Abel inverted version (RHS). Typical features of LX-17 experiments are illustrated.

Time sequence imaging allowed us to examine the onset and evolution of dead-zone formation in LX-17. Figure 5 below is a typical sequence. Here the raw data images are above with the Abel inverted images below. In the first image (0.81 us) the detonation front has just entered the main charge. Close inspection of the data reveal a detonation front and the onset of dead-zone formation. At 2.92 us the detonation is expanding radially and proceeding into the main charge. At 5.13 us the detonation front has finally turned the corner and the detonation has broken out the sides of the main charge. Finally, at 6.63 us, the detonation front is nearly out of the main charge and the dead zone is starting to decompress. Within the observation times of these experiments (22 us) the dead-zones formed in LX-17 persist and never re-initiate. Due to the presence and amount of LX-17 residue post-shot, we conclude that once the dead-zone forms in LX-17, it is never re-initiated or combusted. This is surprising due to the violence of the environment, but TATB is a very insensitive explosive. We find that for LX-17 at 1.91 g/cc the data are consistent with a corner turning time of

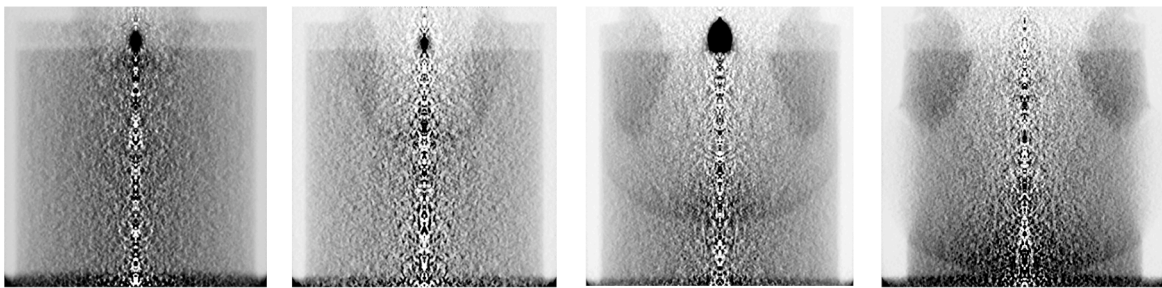
about 3.5 us. This is always true for an initiator to main charge ratio of 1 to 4 with steady state detonation in the booster.

We also evaluated 1.870 g/cc LX-17. Reducing the density increased the corner-turning ability of the detonation and also reduced the dead-zone formed. Corner turning occurred at much earlier times in the lower density charges, at about 1.3 us. Besides the size, the shape of the dead-zone was also affected. This is evident in figure 6 below. Here we compare data from LX-17 at 1.91 g/cc and 1.87 g/cc taken at the same time, 2.9 us. Note that the dead-zone size and shape are drastically different. To quantify this effect, we determined the size of the dead-zone from the radiographs for the two densities. These data are plotted in figure 7. As the dead-zone is a torus, here we plot the cross-sectional area. The 1.91 g/cc data clearly show that the growth of the dead-zone is exponential until corner-turning is achieved. The dead-zone then stagnates and decompresses. Data from the lower density is also plotted here (square data points). The 0.04 g/cc change in density reduces the dead-zone size by a factor of about 4.

Raw Data Images



Abel Inverted Images



0.81 μ s

2.92 μ s

5.13 μ s

6.63 μ s

Notes: Experiment GHG_04_009 (LX-10/LX-17); Times are in relation to timing pin.

Figure 5. Typical LX-17 time sequence image. Upper images are raw data while lower images have been Abel inverted.

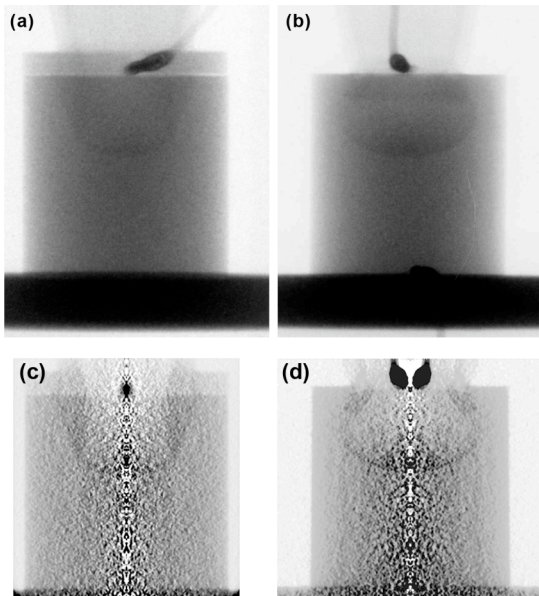


Figure 6. Figures a) and c) are LX-17 density 1.910 g/cc at 2.92 μ s while b) and d) are 1.870 g/cc at 2.94 μ s, essentially the same time.

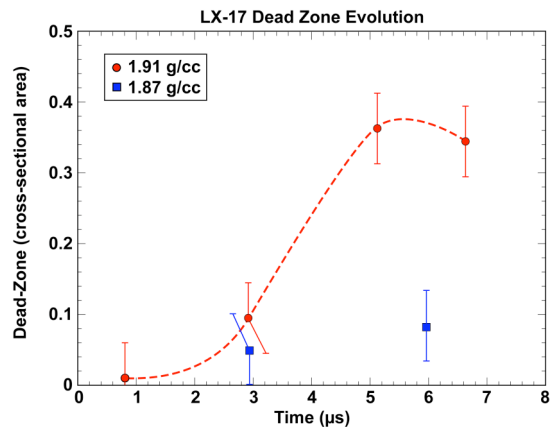


Figure 7. LX-17 dead-zone evolution for both densities studied.

We know that LX-17 dead-zone size and shape are affected by density, but we also have indications that structure within the dead-zone may be affected. At this point we have indications that there is structure within the DZ, but it is at the limit of our resolution and contrast.

Composition B Results

Composition B was important to this research as previous work by Manfred Held using a similar GHG configuration found significant dead-zone formation [2]. We explored detonation corner turning in composition B in pressed form at 1.70 g/cc and in cast form at 1.59 g/cc. These data are

shown below. Figure 8 shows a composition B detonation sequence for the pressed material at 1.70 g/cc. There is no indication of any dead zone formed. The detonation front is clean and sharp and only expanding reaction products are observed behind it.

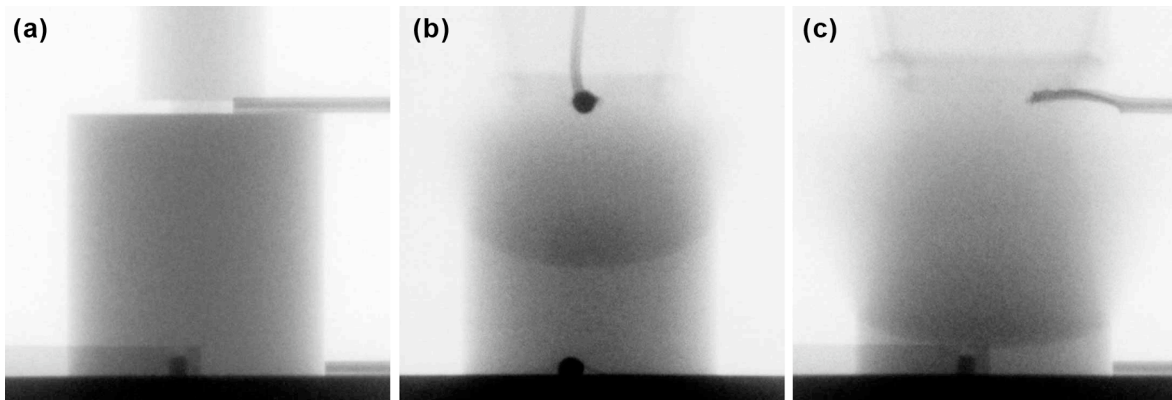


Figure 8. Pressed composition B detonation sequence at 1.70 g/cc. a) static; b) 3.970 us; c) 5.980 us. As image b) is just later than the corner turning time of LX-17, a comparable dead-zone would be visible here.

In figure 9 we show a composition B detonation sequence for a cast main charge of density 1.59 g/cc. Even at early times the detonation front is sharp and shows no indication

of a dead-zone. The lighter regions in the image are void regions due to the casting process, except for the two pressure points in image 9d), which are film artifacts.

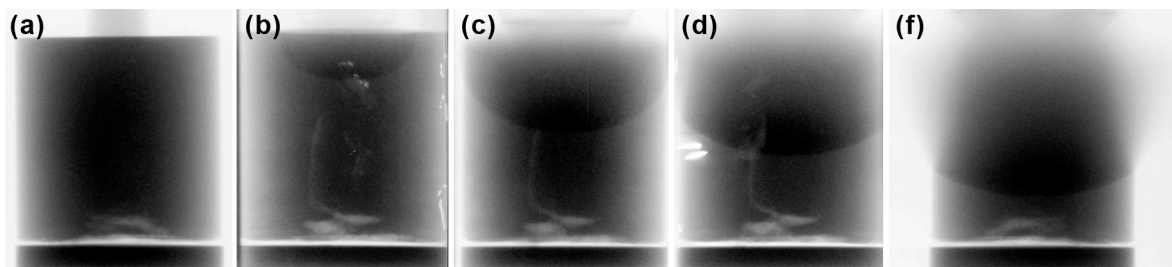


Figure 9. Composition B full time sequence: a) static, b) 1.585 us; c) 6.515 us; d) 8.160 us; f) 10.5 us. All these images were taken on a single shot.

We used our Abel inversion techniques to examine the composition B data. If there was a dead-zone, it should be evident in the earliest time data. Image 9b) was the most likely candidate for any indication of a dead-zone, but the Abel analysis did not reveal anything. A comparison

of the raw and Abel inverted image is shown in figure 10 below. The detonation front is sharp and cleanly dish-shaped in both the raw and Abel inverted data. The Abel inversion also brought out the complex void structure in the main charge and made it more apparent.

The main differences in the work cited here with that of Held [2] was in the Composition B formulation, preparation and main charge densities. Our composition B was 60% RDX and 40% TNT, while Held used different combinations, the closest to ours being 65% RDX and 35% TNT. However all of Held's charges

were higher in density. The 65/35 charge was cast with a density of 1.71 g/cc, which was very close to our 60/40 main charge which was pressed to 1.70 g/cc. The diagnostics used in the two investigations were of course very different. The Hydra radiographs could never have missed the dead-zone observed by Held.

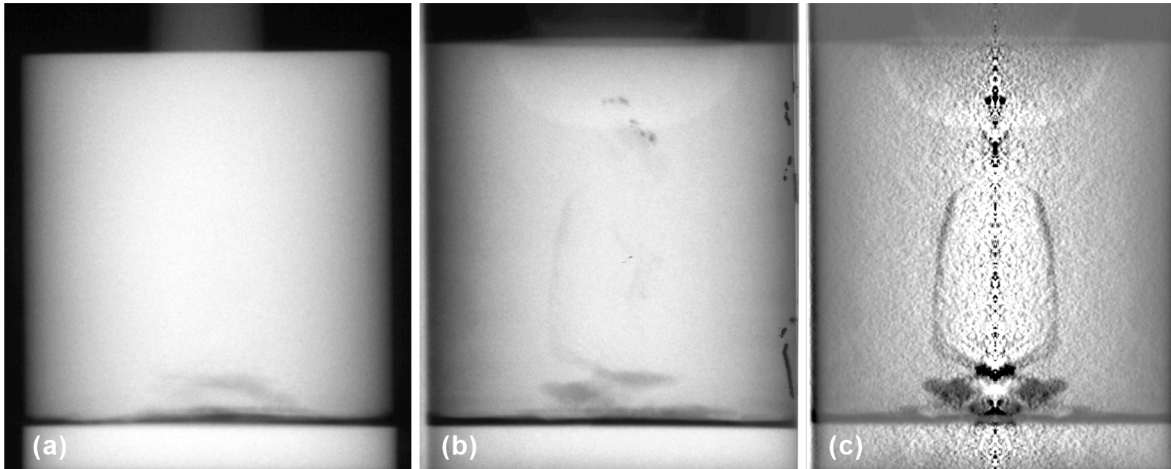


Figure 10. Composition B dead-zone analysis: a) static; b) raw image data; c) Abel inverted data. This analysis did not reveal any indication of a dead-zone in composition B.

Tritonal Results

The tritonal experiment used melt cast material at a density of 1.710 g/cc. In the single experiment performed, corner-turning was not an issue and no dead-zone was observed. However, this experiment was significantly different than the others in that the initiator was pentolite and the diameter ratio was 1 to 3. Finally, the initiator was very short at only one inch in length. Because of these issues, we hope to re-evaluate the corner turning capability of tritonal in the future. We also note that tritonal was the only metalized explosive investigated here and feel that more work should be done in this area.

CONCLUSIONS

We have investigated detonation corner-turning for four high-explosives in a cylindrically symmetric outer-corner configuration known as the German Hand Grenade or GHG configuration. The explosives evaluated were: LX-04, LX-17, Composition B, and Tritonal. Of the 13 experiments performed in this research, LX-17

and Composition B were investigated very thoroughly. LX-17 was the only material that showed an inability of the detonation to successfully corner turn leading to the formation of a dead-zone. As the density of the LX-17 was reduced, so was the dead-zone which formed. One conclusion we draw from this is that dead-zone formation may be possible in any explosive as the density increases and approaches the theoretical maximum. Furthermore, this research showed that the dead-zones in LX-17 persisted and were long lived. In LX-17 there was no evidence that the dead-zone ever re-detonated or even combusted post-detonation. None of the other high-explosives evaluated here showed any issues with detonation corner turning and none exhibited any dead-zone formation. Composition B was examined at two densities, but neither exhibited any indication of corner-turning issues or dead-zone formation. We conclude that dead-zone formation is highly possible in insensitive high-explosives and may be possible in all explosives pressed to higher densities, but further research in this area is warranted.

ACKNOWLEDGEMENTS

We acknowledge the data reduction and computer graphics skills of Sabrina Fletcher, whose help in this effort was very much appreciated. We also gratefully appreciate the efforts of the HEAF operations staff during the course of these experiments, especially Larry Crouch and Brian Cracchiola.

This work was performed under the auspices of the U. S. Department of Energy by University of California, Lawrence Livermore National Laboratory under contract No. W-7405-ENG-48.

REFERENCES

1. Cox, M., Campbell, A. W., "Corner Turning in TATB," *Proceedings of the 7th Detonation Symposium*, pp. 624, Annapolis, MD, June 16-19, 1981.
2. Held, M., "Corner-Turning Distance and Retonation Radius," *Propellants, Explos., Pyrotech.*, 14, 153, 1989.
3. Held, M., "Corner Turning Research Test," *Propellants, Explos., Pyrotech.*, 14, 153, 1989.
4. Souers, P. Clark., Andreski, H. G., Cook, C. F. III, Garza, R., Pastrone, R., Phillips, D., Roeske, F., Vitello, P., and Molitoris, J. D., "LX-17 Corner-Turning," *Propellants, Explos., Pyrotech.*, 29, No. 6, pp 359-367, 2004.
5. Molitoris, J. D., "Fast High-Resolution Radiographic Imaging of Dynamic Experiments with Energetic Materials," *Proceedings of Parari 2005, 7th Australian Explosives Ordnance Symposium*, Melbourne, Australia, November 2005.
6. Souers, P. Clark., Andreski, H. G., Batteux, J., Bratton, B., Cabacungan, C., Cook, C. F. III, Fletcher, S., Garza, R., Grimsley, D., Handly, J., Hernandez, A., McMaster, P., Molitoris, J. D., Palmer, Rick., Prindivelle, J., Rodriguez, J., Schneberk, D., Wong., and Vitello, P., "Dead Zones in LX-17 and PBX 9502," *Propellants, Explos., Pyrotech.*, 31, No. 2, pp 89-94, 2006.
7. Rochester Laboratory for Laser Energetics Report Article. "Abel Inversion of Emission and Backlighting Images," *LLE Review*, Vol. 66, NTIS document No. DOE/SF/19460-17, (unpublished), pp 66-72, 2003.
8. Aufderheide, M. B. III, Vantine, H., Egan, P. O. and Morgan, D., "X-Ray imaging and reconstruction of a detonation front," *Nucl. Instr. And Meth. In Phys. Res. A* 422, pp 704-708, (1999).